J Electr Eng Technol.2018; 13(3): 1110-1122
http://doi.org/10.5370/JEET.2018.13.3.1110

ISSN(Print) 1975-0102
ISSN(Online) 2093-7423

Stochastic Stability Analysis of the Power System Incorporating Wind Power using Measurement Wind Data

Panom Parinya†, Anawach Sangswang*, Krissanapong Kirtikara and Dhirayut Chenvidhya****

Abstract – This paper proposes an alternative method to evaluate the effect of wind power to the power system stability with small disturbance. Alternatively, available techniques for stability analysis of a power system based on deterministic methods are less accurate for high penetration of wind power. Numerical simulations of random behaviors are computationally expensive. A stochastic stability index (*SSI*) is proposed for the power system stability evaluation based on the theory of stochastic stability and energy function, specifically the stochastic derivative of the relative well-defined energy function and the critical energy. The *SSI* is implemented on the modified nine-bus system including wind turbines under different conditions. A doubly-fed induction generator (DFIG) wind turbine is characterized and modeled using measured wind data from several sites in Thailand. Each of the obtained wind power data is analyzed. The wind power effect is modeled considering the aggregated effect of wind turbines. With the proposed method, the system behavior is properly predicted and the stability is quantitatively evaluated with less computational effort compared with conventional numerical simulation methods.

Keywords: Stochastic stability analysis, Power system stability, Small disturbance, Well-defined energy function, Stochastic stability index, Doubly-fed induction generator wind turbine, Geographically distributed wind turbines, Aggregated effect, Numerical simulation method

1. Introduction

The impacts of wind energy generation on the power system are of increasing concerned due to a continual increase of wind energy penetration in many countries, passing the empirical acceptable level of 20% [1]. The cumulative wind power capacity grows by an average of 22% annually since 2001 and reaches 486.8 GW worldwide at the end of 2016 [2]. The onshore wind turbine technology with the most market share to date is the doubly-fed induction generator (DFIG) with a share of more than 50% [3]. The escalation of wind power penetration presents a risk on the power system stability due to random nature of the wind power. This raises the importance of the power system stability analysis with the methods that can accurately capture the random characteristics of wind power.

In typical small disturbance analyses, deterministic methods, such as eigenvalue analysis, have been used in the small signal stability analysis of power systems incorporating wind power [4, 5], and [6]. These methods employ the linearization technique to approximate nonlinear characteristics of the system. However, this method is less accurate for the large variation of loads and intermittent sources. Since the wind power is a stochastic process, analyses based on deterministic approaches may result in a possible misdetection of instability due to the inability to properly capture the random behavior of the wind power [7]. There have been many attempts to include the probabilistic characteristics in the stability analysis [7, 8], and [9]. To find the statistics of eigenvalues, the sensitivity of eigenvalues with respect to wind power has to be numerically determined. Nonetheless, these methods assume sufficiently small disturbance such that the system may be described by a set of linear equations and the non-linear effects are neglected. A probabilistic method such as Monte Carlo simulation has been applied to study the characteristic of the power system [10-12], and [13]. Stochastic differential algebraic equations are also used. This technique combines the numerical integration and Monte Carlo simulation for stability analysis of the power system [14] and [15]. Even though the random effects have been captured in transient stability analysis, they however are computationally expensive.

Alternatively, the stochastic techniques, such as in [16, 17], and [18], have been developed and applied for power systems and power electronics stability analysis. The mean first passage time is proposed as a performance index to evaluate the stability of the system [19]. This technique is

† Corresponding Author: The Joint Graduate School of Energy and Environment, Thailand. (panom.par@kmutt.ac.th)
* Department of Electrical Engineering, Faculty of Engineering, King Mongkut's University of Technology Thonburi, Thailand. (anawach.san@kmutt.ac.th)
** CES Solar Cells Testing Center, King Mongkut's University of Technology Thonburi, Thailand. ({ikrikara, dhirayut.che}@kmutt.ac.th)
Received: December 14, 2016; Accepted: February 1, 2018

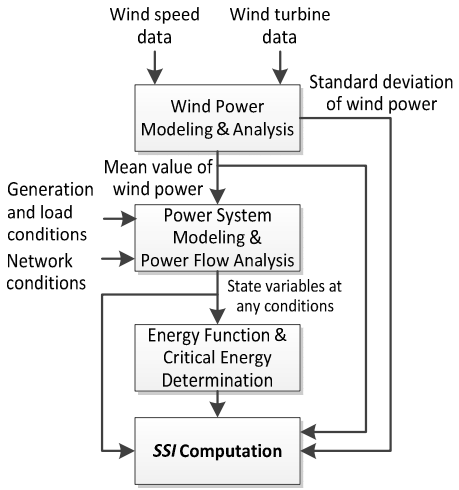

Fig. 1. *SSI* computational process

based on a simplified (quadratic) energy function and successfully applied with power systems with synchronous machines. There has been a study of the effect of induction generator wind turbine using stochastic stability index (*SSI*) with a simplified induction generator model [20]. To properly address the DFIG, this paper studies the effects of stochastic wind power to the power system stability using an improved *SSI* which is a relative stability index. A simplified model of DFIG wind turbine is used in the stability analysis with the standard three-machine, nine-bus power system [21]. A sample of measured wind data in Thailand is first examined for the *SSI* evaluation. The *SSI* computational process can be summarized as shown in Fig. 1. The wind speed and turbine data are used with the wind power modeling to obtain the mean and standard deviation values of the wind power. Then the power flow calculation is performed using the mean wind power along with other network conditions. The state variables are used to determine the critical energy. The *SSI* is computed using the critical energy, state variables at test conditions, along with the mean and standard deviation values of wind power.

The paper is organized as follows: Section 2 describes the wind power characteristics. Section 3 explains the wind power and power system models. Section 4 discusses the concept of stochastic stability analysis and the proposed method. The *SSI* computation results of the nine-bus standard test system are provided in section 5. Finally, the conclusion is given in section 6.

2. Characteristics of Wind Power

The wind power characteristics are studied in this section. With a measurement station setup, the wind data have been collected and analyzed. To characterize the wind power, an appropriate model is chosen to accurately describe the effects of wind power on the power system.

2.1 Wind power components

The dynamics of wind speed consist of two main components, the slow variation component with spectral ranges between 10 hours and several months, and the turbulence components with spectral ranges from 1 second to 10 minutes [22]. The slow variation wind component is influenced by the diurnal and seasonal meteorological effects and can be modeled statistically using Weibull distributions. The turbulence component can be modeled as a zero mean random process [23]. As a consequence, the wind power also consists of slow variation and fast variation components. The slow variations of wind power (P_{ws}) are influenced by the slow variation component of wind speed. The fast variations are influenced by the turbulence of wind speed and the dynamics of wind turbines. The decomposition of fast variations wind power (P_{wf}) are the low frequency component (frequencies up to 0.5Hz) relating to the turbulence wind speed and the high frequency (frequencies above 0.5Hz) component relating to the dynamics of wind turbine [24]. The contribution of low frequency wind power variations (P_{wl}) is about 16 – 22% of the rated capacity. The high frequency component (P_{wh}) is only about 2% [24]. Therefore, the effect of high frequency power variation is essentially negligible.

The wind power (P_w) can be expressed as,

$$P_w = P_{ws} + P_{wf} \approx P_{ws} + P_{wl} \tag{1}$$

2.2 Measurement of wind data

A collection of wind speed data has been obtained from 7 wind monitoring stations in various regions of Thailand, 6 stations (S1 to S6) with 90-meter height located in the Northeastern Thailand and another station (S7) with 120-meter height located in Bangkok as shown in Fig. 2. The siting locations are chosen based on the wind power potential. The wind turbines are located at the same place as the wind monitoring stations. The wind power is then calculated using the sampled wind speed data and the power curve of the 2.3 MW Siemens SWT2.3-101 wind turbine, commonly found DFIG wind turbines installed in Northeastern Thailand. Fig. 3 shows sampled data of wind speed and power at 120-meter height obtained from the S7 wind monitoring station in Bangkok. The wind speed is measured every second while the hourly data is evaluated from the averaged values of the measured wind speed data. It can be seen that the hourly average wind speed and wind power (slow wind power variation or P_{ws}) are modulated by the 1-second wind speed and wind power (fast wind power variation or P_{wf}), respectively. The contribution of the P_{wf} is mainly from a turbulence of wind speed which can be approximated by using the zero-mean normal distribution [25]. The data distributions of 6 equivalent wind turbines are illustrated in Fig. 4. The sum of 6 geographically distributed wind turbines is shown in Fig. 5.

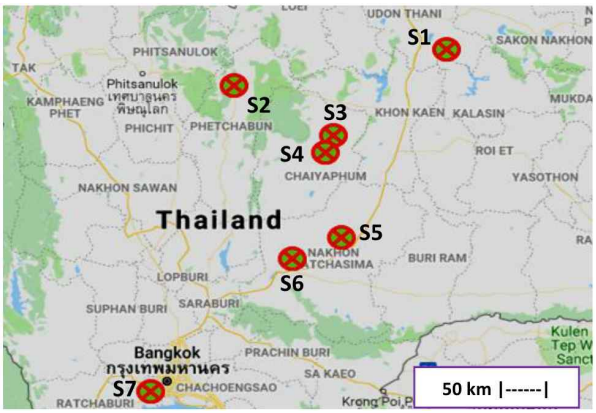

Fig. 2. The locations of 7 wind monitoring stations (S1 to S7)

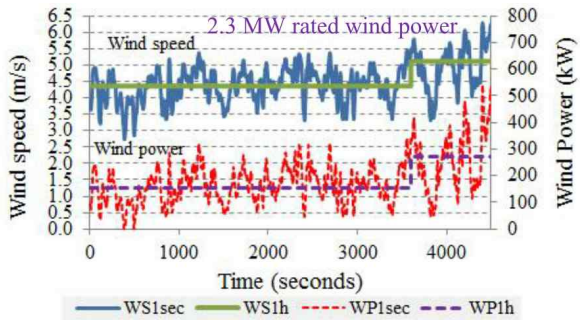

Fig. 3. Sampled data of 1-second (1sec) and hourly (1h) wind speed (WS) and wind power (WP) at the S7 station

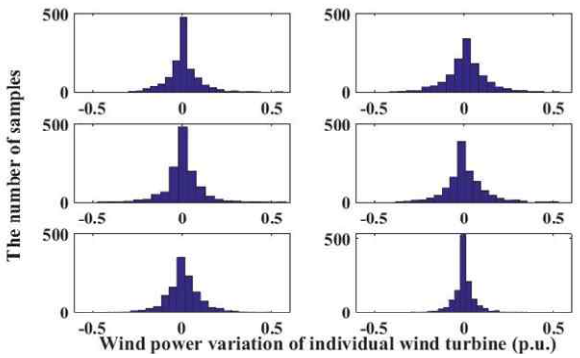

Fig. 4. Histogram of wind power variation of 6 equivalent wind turbines with zero mean Laplace distribution

Each wind turbine is an equivalent representative of a wind farm. The fast wind power variations can be characterized by the zero mean Laplace distribution [26] as shown in Fig. 4. The total effect of 6 geographically distributed wind turbines is comparable with normal distribution data (red line) as shown in Fig. 5. To verify this assumption, the hypothesis for normal distribution of wind power variation data is tested using the Kolmogorov-Smirnov hypothesis test method [27] with significance level at 0.05 (excluding calm winds). The Kolmogorov-Smirnov test evaluates the null hypothesis that the data

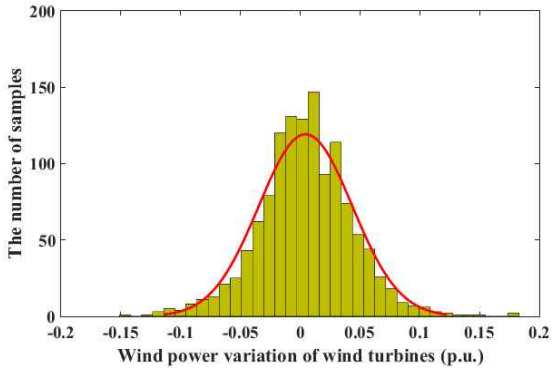

Fig. 5. Histogram of wind power variations of the sum of 6 geographically distributed wind turbines compared with normal distribution data (red line)

Table 1. Kolmogorov-Smirnov hypothesis test results of 6 equivalent wind turbines and the total effect of all turbines

Wind turbine station	Significant level = 0.05	Meaning
S1	H = 1	Reject null hypothesis
S2	H = 1	
S3	H = 1	
S4	H = 1	
S5	H = 1	
S6	H = 1	
Sum of S1 to S6	H = 0	Accept null hypothesis

distribution of wind power variation is comparable to normal distribution. The results in Table 1 indicate that the Kolmogorov–Smirnov test accepts the null hypothesis which means there is no significant difference between the distribution of wind power variation and normal distribution. Since there is no evidence to counter the normal distribution hypothesis of the fast variation wind power, the random effect of wind power of the geographically distributed wind turbines is treated as a Wiener process in this work.

The strength of the random perturbations inherent in the wind power may be reflected through noise intensity (α_w) which is defined as,

$$\alpha_w = \frac{\sigma}{\mu} \tag{2}$$

where σ and μ are standard deviation and mean values, respectively.

The noise intensity depends mainly on local wind characteristics and weathers. For example, the yearly noise intensity of four wind power plants in USA during 2000 to 2010 varies as large as 0.8 to 1.0 [28]. In this study, it is calculated from the hourly average wind power and its standard deviation. An increase of noise intensity due to higher standard deviation value implies that the wind power is highly fluctuated and is subjected to power system instability. The higher noise intensity, the greater

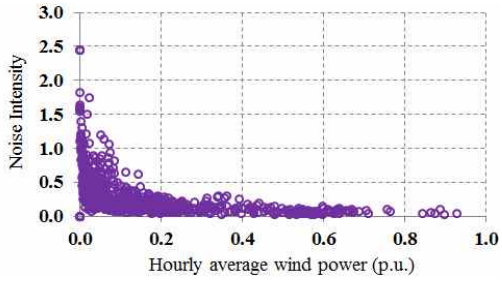

Fig. 6. Relationship between the hourly average wind power and noise intensity of 6 wind turbines

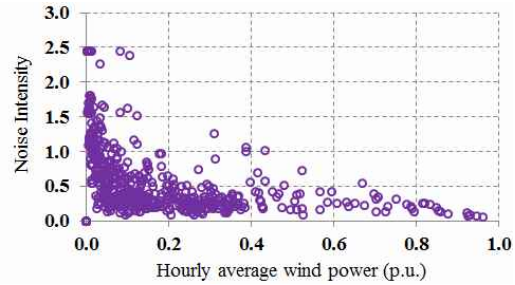

Fig. 7. Relationship between the hourly average wind power and noise intensity of equivalent wind turbine

variation of the wind power as given in (2).

Statistical data of the total effect of 6 geographically distributed wind turbines and equivalent wind turbine (Station S3) are shown in Fig. 6 and 7, respectively. In Fig. 6, at the noise intensity higher than 0.5, most of the wind power values are lower than 0.2 p.u. and decreased as the wind power increases. The noise intensity in Fig. 7 is rather scattered and greater than those in Fig. 6 for the same value of wind power.

2.3 The wind power noise model

As mentioned earlier, the wind power (P_w) is composed of the slow and fast variation components. The slow variation part is assumed to be constant within a sustained period, namely, one hour. The fast variation component can be approximated with the zero-mean Gaussian distributed white noise. The white noise is assumed in this study to allow the inclusion of the actual spectral density in the stochastic differential equations. The wind power is represented by the per unit mechanical wind power ($\overline{P}_{mw}$) as the input of the generator. Therefore, the $\overline{P}_{ws}$ in (1) is replaced by the $\overline{P}_{mws}$ and the $\overline{P}_{wl}$ is replaced by $\overline{P}_{mwl}$ and can be stated as follows (over bar represents per unit value):

$$\overline{P}_{mw} = \overline{P}_{mws} + \overline{P}_{mwl} \tag{3}$$

where $\overline{P}_{mws}$ is the slow variation component of $\overline{P}_{mw}$ and is assumed constant. The $\overline{P}_{mwl}$ is the low frequency variation component of $\overline{P}_{mw}$ and is approximated with the zero-mean Gaussian distributed white noise. The expression in (3) becomes:

$$\overline{P}_{mw} = \overline{P}_{mws}\left(1+\alpha_w \dot{W}\right) \tag{4}$$

where $\dot{W}$ is a zero-mean Gaussian distributed white noise [19]. Therefore, the wind power characteristics and the wind power noise model in (4) are used in wind power modeling detailed in the next section.

3. Wind Power and Power System Modeling

3.1 DFIG wind turbines model

For the DFIG wind turbine, the stator is directly connected to the grid while the rotor winding is connected through the back-to-back converter for speed, torque, and output voltage regulations [5] as shown in Fig. 8. The converter is typically consisted of two AC/DC IGBT-based voltage source converters (VSCs), linked through a DC bus with DC capacitor (C_{DC}). When the generator operates in super-synchronous mode, the power is delivered from the rotor to the network through the converters. When the generator operates in sub-synchronous mode, the rotor absorbs power from the network through the converters [5].

The key component of the DFIG turbine is the speed-torque characteristic which has direct effect on the synchronizing stability. The rotor dynamic relation between the torque balance and frequency deviation of the DFIG are provided as follows [5]:

$$\mathrm{d}\left(\omega_{rw}/\omega_{sw}\right)/\mathrm{d}t = \Delta\dot{\overline{\omega}}_w = -\dot{s}_w = M_w^{-1}\left(\overline{P}_{mw} - \overline{P}_{ew}\right) \tag{5}$$

where the subscript w represents the DFIG wind turbines and the over bar represents the per unit values.

The voltage deviation equation of DFIG in the x-y or system reference axis can be represented in (6) which is modified from [5, 29], and [30]. The rotor voltage ($\overline{\mathbf{V}}_r$), voltage behind transient reactance ($\overline{\mathbf{E}}$'), and stator current ($\overline{\mathbf{I}}_s$) are complex numbers.

$$\left.\begin{aligned} \dot{\overline{\mathbf{E}}}' &= -\overline{T}_0^{-1}\left(\overline{\mathbf{E}}' + j\left(\overline{X}-\overline{X}'\right)\overline{\mathbf{I}}_s\right) - js_w\omega_s\overline{\mathbf{E}}' + j\omega_s\overline{\mathbf{V}}_r\overline{L}_m\overline{L}_{rr}^{-1} \\ \overline{\mathbf{E}}' &= \left|\overline{E}'\right|e^{j\delta_w}, \qquad \overline{\mathbf{V}}_r = \left(V_{rq} - jV_{rd}\right)e^{j\delta_w} \\ \overline{\mathbf{I}}_s &= \left(I_{sq} - jI_{sd}\right)e^{j\delta_w}, \qquad \overline{T}_0 = \overline{L}_{rr}\omega_0^{-1}\overline{r}_r^{-1} \end{aligned}\right\} \tag{6}$$

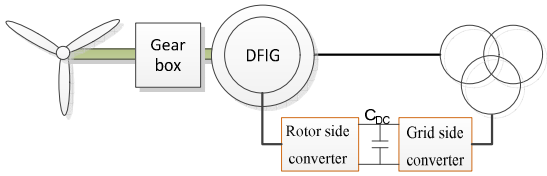

Fig. 8. DFIG wind turbine diagram

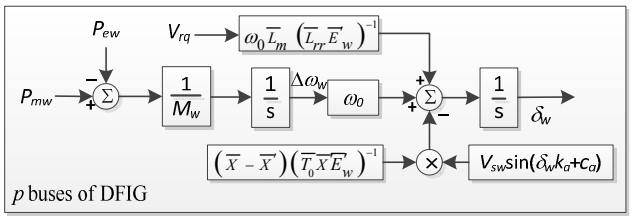

Fig. 9. Simplified DFIG wind turbine model

Note that the last term of the first row in (6) is zeroed out in the case of classical induction generators. The derivative of $\overline{\mathbf{E}}$**'** in (6) can be separated into the derivative of $|\overline{E}'|$ and δ_w. The derivative of $|\overline{E}'|$ (or simply $\overline{E}'$) is sufficiently small and negligible and (6) becomes:

$$\left.\begin{aligned}\dot{\delta}_w &= -\left(\overline{X}-\overline{X}'\right)\left(\overline{T}_0\overline{X}\overline{E}'_w\right)^{-1}\overline{V}_{sw}\sin\delta'_w - s_w\omega_{sw}+\omega_{sw}\overline{L}_m\left(\overline{L}_{rr}\overline{E}'_w\right)^{-1}\overline{V}_{rq}\\ \delta'_w &= k_a\delta_w + c_a \quad [20]\\ k_a &= 0.274\overline{P}_{mws}+0.346, \quad c_a = -0.022\overline{P}_{mws}+0.006\end{aligned}\right\} \tag{7}$$

The other variables in (7) can be stated as follows:

$$\left.\begin{aligned}\overline{V}_{rq} &= s_w\left(k_{c1}\overline{E}'_w + k_{c2}\overline{V}_{sw}\cos\delta'_w\right)+k_p\left(\overline{T}_{sp}-\overline{P}'_{sw}\right)+k_w\\ \overline{T}_{sp} &\approx k_{op}\omega_{rw}^2 = k_{op}\left(1-s_w\right)^2 \text{ and } \overline{P}'_{sw}\approx k_m\overline{P}_{ew}/\left(1+s_w\right)\end{aligned}\right\} \tag{8}$$

$$\left.\begin{aligned}k_{c1} &= \overline{\omega}_0\left(\overline{L}_{rr}-\overline{L}_m^2/\overline{L}_{ss}\right)\left(\overline{L}_{ss}/\overline{L}_m\overline{X}'\right)\\ k_{c2} &= \overline{\omega}_0\left(\left(\overline{L}_{rr}-\overline{L}_m^2/\overline{L}_{ss}\right)\left(1/\overline{\omega}_{sw}\overline{L}_m-\overline{L}_{ss}/\overline{L}_m\overline{X}'\right)+\overline{L}_m/\overline{\omega}_{sw}\overline{L}_{ss}\right)\end{aligned}\right\} \tag{9}$$

where k_w is very small compared with k_p and negligible [5].

Therefore, the DFIG wind turbine model is simplified and represented by the second-order model consisting of two differential equations in (5) and (7) as represented in Fig 9. In this figure, the rotor speed deviation ($\Delta\omega_w$) depends on the power imbalance between $\overline{P}_{mw}$ and $\overline{P}_{ew}$. The rotor angle (δ_w) depends on the speed deviation, stator voltage ($\overline{V}_{sw}$), and rotor voltage ($\overline{V}_{rq}$).

3.2 The power system equations

The power system in this study is the lossless structure preserving model from [16] which consists of an *n*-bus power system with *m* generator buses (*p* buses of DFIG and *m*-*p* buses of synchronous generators) and *n*-*m* load buses. The power system equations with wind turbine models from (5) and (7) are given as follows:

$$M_i\Delta\dot{\overline{\omega}}_i = \left(\overline{P}_{mi}-\overline{P}_{ei}\right)-D_i\Delta\overline{\omega}_i \tag{10}$$

$$\dot{\delta}_i = \omega_0\left(\overline{\omega}_r-\overline{\omega}_s\right)=\omega_0\Delta\overline{\omega}_i \tag{11}$$

$$M_w\Delta\dot{\overline{\omega}}_w = \left(\overline{P}_{mw}-\overline{P}_{ew}\right) \tag{12}$$

$$\left.\begin{aligned}\dot{\delta}_w &= \omega_0\Delta\overline{\omega}_w - k_b\overline{V}_{sw}\sin\left(k_a\delta_w+c_a\right)+\omega_0 k_d\overline{V}_{rq}\\ k_d &= \overline{L}_m\left(\overline{L}_{rr}\overline{E}'_w\right)^{-1},\quad k_b=\left(\overline{X}-\overline{X}'\right)\left(\overline{T}_0\overline{X}\overline{E}'_W\right)^{-1}\end{aligned}\right\} \tag{13}$$

$$c_k\dot{\theta}_k = -\left(\overline{P}_{lk}+\overline{P}_{ek}\right)-c_k\omega_0 \tag{14}$$

$$\overline{P}_{ew} = \overline{E}'_w\sum_{j=1,j\neq w}^{n}\overline{V}_j\overline{B}_{wj}\sin\left(\delta_w-\theta_j\right) \tag{15}$$

$$\overline{P}_{ei} = \overline{V}_i\sum_{j=1,j\neq i}^{n}\overline{V}_j\overline{B}_{ij}\sin\left(\delta_i-\theta_j\right) \tag{16}$$

$$\overline{P}_{ek} = \overline{V}_k\sum_{j=1,j\neq k}^{n}\overline{V}_j\overline{B}_{kj}\sin\left(\theta_k-\theta_j\right) \tag{17}$$

where ω_s can be replaced by ω_0. The subscript *i*, *w*, and *k* represent synchronous generators, DFIGs wind turbine, and load buses, respectively.

3.3 The perturbed-system model

To represent the dynamic perturbed system equations [16], the following substitutions are made,

$$\left.\begin{aligned}\varphi_{df}\left(\mathbf{V},\mathbf{x}\right) &= \omega_0 k_d\overline{V}_{rq}-k_b\overline{V}_{sw}\sin\left(k_a\left(x_w-x_{ref}\right)+c_a\right)\\ \varphi_k\left(\mathbf{V},\mathbf{x}\right) &= -\frac{1}{c_k}\left(\overline{P}_{lk}+\overline{P}_{ek}\right)-\omega_0 y_0\\ \varphi_i\left(\mathbf{V},\mathbf{x}\right) &= \frac{1}{M_i}\left(\overline{P}_{mi}-\overline{P}_{ei}\right)\\ \varphi_w\left(\mathbf{V},\mathbf{x}\right) &= \frac{1}{M_w}\left(\overline{P}_{mw}-\overline{P}_{ew}\right)\end{aligned}\right\} \tag{18}$$

The mechanical power ($\overline{P}_{mw}$) in (12) is replaced by (4), the power system equations in (10) to (14) are rearranged to become a standard diffusion process as follows:

$$\frac{\mathrm{d}}{\mathrm{d}t}\begin{bmatrix}x_i\\x_w\\x_k\\y_i\\y_w\end{bmatrix} = \begin{bmatrix}\omega_0\left(y_i-y_0\right)\\ \omega_0\left(y_w-y_0\right)+\varphi_{df}\left(\mathbf{V},\mathbf{x}\right)\\ \varphi_k\left(\mathbf{V},\mathbf{x}\right)\\ \varphi_i\left(\mathbf{V},\mathbf{x}\right)-\beta_i y_i\\ \varphi_w\left(\mathbf{V},\mathbf{x}\right)\end{bmatrix} + \begin{bmatrix}0\\0\\0\\0\\ \dfrac{P_{mw}\alpha_w}{M_w}\end{bmatrix}\frac{\mathrm{d}W}{\mathrm{d}t} \tag{19}$$

where $\beta_i = D_i/M_i$. The power system equations are used to formulate the energy function and its derivative while the standard diffusion process form is used to formulate the stochastic energy function as in the following section.

4. Proposed Stochastic Stability Analysis

4.1 Stochastic stability

The energy function based on the direct method can provide a quantitative measure of degree of power system

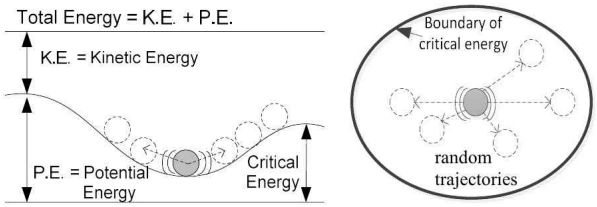

Fig. 10. System energy from side (left) and top views (right)

stability without performing the time-consuming numerical integration [31]. Therefore, the energy function is adopted for power system stability evaluation in this work. The energy function and critical energy are generally known for the deterministic system but it is not the case for a stochastic system. A rolling ball on a hill may be used to illustrate trajectories of the system states as shown in Fig. 10. The grey ball represents a particular system operating point. When the system is perturbed, the system states are changed and the system energy is increased. Once the system energy is greater than the critical energy, the system essentially becomes unstable. Unlike deterministic systems, the trajectories of states in the stochastic system are random and not repeatable. Conventional deterministic approaches in stability analysis may not be appropriate. However, the boundaries of stability of both deterministic and stochastic systems remain the same. It means that the critical energy can be used as the boundary of the stochastic system.

From the theory of stochastic stability, without corrective action, the trajectories of any continuously perturbed system will diverge from the origin to the arbitrarily large distances with probability one in finite time even under an influence of small perturbation [19]. Thus the principle of the stochastic stability is to estimate the energy that the system may reach compared with the system energy at the boundary of the stable region. Since the trajectories of states are random, the system energy function is used to formulate the stochastic measure which will be described in following sections.

4.2 Energy function

An energy function has been used as a Lyapunov function candidate in many cases. For a single-machine power system, the energy function can be established as a positive definite function and used as a Lyapunov function. However, this is not the case for a multi-machine power system where the energy function possesses terms with indefinite sign. Alternatively, the well-defined energy function conditions have been imposed to evaluate the stability of the power system for the direct method [31]. The positive definite requirement of the Lyapunov function is relaxed such that the definite sign condition on the Lyapunov function is removed. For the nonlinear system with time invariant and force free, the conditions for the well-defined energy function are as follows [31]:

- The derivative of well-defined energy function along any system trajectory is non-positive.
- The derivative of energy function is zero when the operating points (state variables) are the equilibrium points.
- The well-defined energy function is bounded which means state variables are also bounded.

These three conditions are considered in the relative well-defined energy function (U) formulation using the first integral method in [31] and [32]. and are provided as follows:

$$\frac{\mathrm{d}}{\mathrm{d}t}\left[\begin{array}{l}\sum_{i=1}^{m-p}\frac{1}{2}\omega_0 M_i y_i^2-\sum_{i=1}^{m-p}\bar{P}_{mi}x_i-\sum_{\substack{w=m\\-p+1}}^{m}\bar{P}_{mw}x_w+\sum_{k=m+1}^{n}P_{lk}x_k\\+\sum_{\substack{w=m\\-p+1}}^{m}\frac{1}{2}\omega_0 M_w y_w^2-\sum_{\substack{w=m\\-p+1}}^{m}\int_{y_{0w}}^{y_w}\left[M_w k_b V_{sw}\sin\left(k_a\left(x_w-x_{ref}\right)+c_a\right)\right]\mathrm{d}y_w\\+\sum_{\substack{w=m\\-p+1}}^{m}\int_{y_{0w}}^{y_w}\left[M_w\omega_0 k_d\left(\begin{array}{l}k_P k_{op}\left(y_w+1\right)^2-k_P k_m\bar{P}_{ew}\left(1+y_w\right)^{-1}\\-y_w\left(k_{c2}\bar{V}_{sw}\cos\left(k_a\left(x_w-x_{ref}\right)+c_a\right)+k_{c1}\bar{V}_w\right)\end{array}\right)\right]\mathrm{d}y_w\\-\sum_{i=1}^{n-1}\sum_{j=i+1}^{n}V_i V_j B_{ij}\cos\left(x_i-x_j\right)+K\end{array}\right]$$
$$=-\sum_{i=1}^{m-p}\omega_0 D_i y_i^2-\sum_{k=m+1}^{n}c_k\dot{x}_k^2+\omega_0 y_0\left(\sum_{i=1}^{m}P_{mi}-\sum_{j=1}^{m}P_{ej}-\sum_{k=m+1}^{n}c_k\dot{x}_k\right) \quad (20)$$

The left-hand side in (20) is the derivative of U of the power system where the constant K is defined such that U is equal to zero at a stable equilibrium point ($y_j = y^s_j$ and $x_j = x^s_j$), where

$$K=\left\{\begin{array}{l}-\sum_{i=1}^{m-p}\frac{1}{2}\omega_0 M_i y_i^{s2}+\sum_{i=1}^{m-p}\bar{P}_{mi}x_i^s+\sum_{\substack{w=m\\-p+1}}^{m}\bar{P}_{mw}x_w^s-\sum_{k=m+1}^{n}P_{lk}x_k^s\\-\sum_{\substack{w=m\\-p+1}}^{m}\frac{1}{2}\omega_0 M_w y_w^{s2}+\sum_{\substack{w=m\\-p+1}}^{m}\int_{y_{0w}}^{y_w^s}\left[M_w k_b V_{sw}\sin\left(k_a\left(x_w-x_{ref}\right)+c_a\right)\right]\mathrm{d}y_w\\-\sum_{\substack{w=m\\-p+1}}^{m}\int_{y_{0w}}^{y_w^s}\left[M_w\omega_0 k_d\left(\begin{array}{l}k_P\left(k_{op}\left(y_w+1\right)^2-k_m\bar{P}_{ew}\left(1+y_w\right)^{-1}\right)\\-y_w\left(k_{c2}\bar{V}_{sw}\cos\left(k_a\left(x_w-x_{ref}\right)+c_a\right)+k_{c1}\bar{V}_w\right)\end{array}\right)\right]\mathrm{d}y_w\\+\sum_{i=1}^{n-1}\sum_{j=i+1}^{n}V_i V_j B_{ij}\cos\left(x_i^s-x_j^s\right)\end{array}\right\} \quad (21)$$

From (20), the derivative of U can be stated as:

$$\frac{\mathrm{d}U}{\mathrm{d}t}=-\sum_{i=1}^{m-p}\omega_0 D_i y_i^2-\sum_{k=m+1}^{n}c_k\dot{x}_k^2+\omega_0 y_0\left(\sum_{j=1}^{m}\bar{P}_{mj}-\sum_{j=1}^{m}\bar{P}_{ej}-\sum_{k=m+1}^{n}c_k\dot{x}_k\right) \quad (22)$$

where j denotes generator buses including both synchronous and induction generators. In general, it is rather difficult to show that the relationship in (22) is

negative definite since the last term often becomes positive at any particular operating point. However, for the case of a power system with an infinite bus, y_0 is zero and the last term of (22) is diminished. The derivative of U becomes:

$$\frac{\mathrm{d}U}{\mathrm{d}t} = -\sum_{i=1}^{m-p} \omega_0 D_i y_i^2 - \sum_{k=m+1}^{n} c_k \dot{x}_k^2 \tag{23}$$

Therefore, for the deterministic system, the derivative of U is the negative semi-definite function. With a substitution of (21) in (20) and solving the integral terms using the trapezoidal rule, the general form of energy function (U) is given as,

$$\begin{aligned} U = {} & \frac{1}{2}\sum_{i=1}^{m-p} \omega_0 M_i y_i^2 + \frac{1}{2}\sum_{w=m-p+1}^{m} \omega_0 M_w \left(y_w^2 - y_w^{s2}\right) - \sum_{i=1}^{m-p} \bar{P}_{mi}\left(x_i - x_i^s\right) \\ & - \sum_{w=m-p+1}^{m} \bar{P}_{mw}\left(x_w - x_w^s\right) + \sum_{k=m+1}^{n} P_{lk}\left(x_k - x_k^s\right) \\ & - \sum_{\substack{w=m \\ -p+1}}^{m} \frac{1}{2} M_w k_b V_{sw} \begin{pmatrix} \sin\left(k_a\left(x_w - x_{ref}\right) + c_a\right) \\ + \sin\left(k_a\left(x_w^s - x_{ref}\right) + c_a\right) \end{pmatrix} \left(y_w - y_w^s\right) \\ & + \sum_{\substack{w=m \\ -p+1}}^{m} \frac{1}{3} M_w \omega_0 k_d k_P k_{op} \left(\left(y_w + 1\right)^3 - \left(y_w^s + 1\right)^3\right) \\ & - \sum_{\substack{w=m \\ -p+1}}^{m} \frac{1}{2} M_w \omega_0 k_d k_P k_m \left(\bar{P}_{ew} + \bar{P}_{ew}^s\right)\left(\ln\left(y_w + 1\right) - \ln\left(y_w^s + 1\right)\right) \\ & - \sum_{\substack{w=m \\ -p+1}}^{m} \frac{1}{2} M_w \omega_0 k_d k_{c1} \bar{V}_w \left(y_w^2 - y_w^{s2}\right) \\ & - \sum_{\substack{w=m \\ -p+1}}^{m} \frac{1}{4} M_w \omega_0 k_d k_{c2} \bar{V}_{sw} \begin{pmatrix} \cos\left(k_a\left(x_w - x_{ref}\right) + c_a\right) \\ + \cos\left(k_a\left(x_w^s - x_{ref}^s\right) + c_a\right) \end{pmatrix} \left(y_w^2 - y_w^{s2}\right) \\ & - \sum_{i=1}^{n-1} \sum_{j=i+1}^{n} \bar{V}_i \bar{V}_j \bar{B}_{ij} \left[\cos\left(x_i - x_j\right) - \cos\left(x_i^s - x_j^s\right)\right] \end{aligned} \tag{24}$$

The critical energy is used as the boundary of stability of the power system. If the system has gained an excess energy beyond the critical value when perturbed by any disturbance, the system becomes unstable. For convenience, the critical energy (U_c) can be estimated using the method laid out in [33] which requires determination of the energy function, stable equilibrium points, and unstable equilibrium points. Note that the unstable equilibrium points in terms of the phase angles can be approximated using the value $\pm\pi - x^s$ where x^s is the stable equilibrium point [16].

4.3 Stochastic stability index

From the standard diffusion process form in (19), if there exists a positive definite $v(\mathbf{X}, t)$ function with continuous partial derivatives, the system is said to be stable in the sense of Lyapunov providing that [34]:

$$\mathrm{E}\left[\mathrm{d}v\right] \le 0 \quad \text{for all} \quad t \ge t_0 \tag{25}$$

where E[.] is the expected value of the function. The function v is qualified as a Lyapunov function belonging to a particular equilibrium state of the stochastic differential equations [34].

Alternatively, the stochastic well-defined energy function ($u(\mathbf{X}, t)$) is proposed to replace $v(\mathbf{X}, t)$ although it is not the positive definite function as be described in the previous section. The differentiation of $u(\mathbf{X}, t)$ can be stated as follows:

$$\mathrm{d}u\left(\mathbf{X},t\right) = \left(\mathrm{L}u\left(\mathbf{X},t\right)\right)\mathrm{d}t + \sum_{i=1}^{d}\sum_{j=1}^{m} u_{ij}\left(\mathbf{X},t\right) g_{ij}\left(\mathbf{X},t\right)\mathrm{d}W_j \tag{26}$$

The L operator is the Itô differential operator which is represented by,

$$\mathrm{L}\left(.\right) = \frac{\partial\left(.\right)}{\partial t} + \sum_{i=1}^{n} \frac{\partial\left(.\right)}{\partial x_i} \mathrm{f}_i\left(\mathrm{x},t\right) + \frac{1}{2}\left[\sum_{j=1}^{n}\sum_{i=1}^{n} g_i\left(\mathrm{x},t\right) g_j\left(\mathrm{x},t\right) \frac{\partial^2\left(.\right)}{\partial x_i \partial x_j}\right] \tag{27}$$

A substitution of the energy function (U) in (24) in the L operator in (27) results in the LU terms consisting of the time derivative, first-order, and second-order derivatives, known as a trace function (LU_t).

To simplify the calculation in the stability analysis, the following assumptions are made. First, U is a time invariant function and its partial derivative with respect to time is zero. Second, the initial state of the state variables is at equilibrium in which the first-order derivative terms are negligible. As a result, the expectation of (26) can be approximated as follows:

$$\left.\begin{aligned} & \mathrm{E}\left[\mathrm{d}u\left(\mathbf{X}\right)\right] = \mathrm{E}\left[\left(\mathrm{L}u\left(\mathbf{X}\right)\right)\mathrm{d}t\right] \approx \mathrm{L}U = \frac{\mathrm{d}U}{\mathrm{d}t} + \mathrm{L}U_t \\ & \text{where} \quad \frac{\mathrm{d}U}{\mathrm{d}t} = \frac{\partial U}{\partial t} + \sum_{i=1}^{n} \frac{\partial U}{\partial x_i} f_i\left(x_i,t\right) \quad \text{and} \\ & \mathrm{L}U_t = \frac{1}{2}\left[\sum_{j=1}^{n}\sum_{i=1}^{n} g_i\left(x_i,t\right) g_j\left(x_j,t\right) \frac{\partial^2 U}{\partial x_i \partial x_j}\right] \end{aligned}\right\} \tag{28}$$

Note that LU_t in (28) includes the diffusion function $g(x,t)$ and also represents the rate of change of stochastic energy. The larger LU_t, the faster the system energy increases in which it can then reach the critical energy (U_c).

To evaluate the effects of the wind power on the power system, a stability index is proposed. The critical energy and the trace function LU_t are incorporated.

The index is a representation of how long the system energy takes to reach the critical value. Thus, the proposed stochastic stability index (SSI) is defined as follows:

$$SSI = U_c / \mathrm{L}U_t \tag{29}$$

The SSI represents similar concept to the mean first

passage time or the mean first exit time which is the performance index to quantify the average time that a state-space trajectory takes to change from a given operating point to the boundary of domain of attraction under an influence of small perturbations [18]. The *SSI* can be used to compare the robustness of a given power system with random perturbations including system power perturbed by wind power, load and power balance. The power system stability is more robust for a larger *SSI*. A higher *SSI* is due to a higher critical energy or lower trace function. That is a large value of energy is needed to push the system out of the domain of attraction. In other word, the system is more robust to the cumulative effect of the fluctuated wind power. To compute the *SSI*, the power, phase voltage, and angle at steady-state condition and network matrices of the power test system are evaluated using the relationships in (10) to (19). The critical energy is obtained from (24) and the trace function is obtained from (28) using state variables at steady-state condition.

5. Stochastic Stability Index Evaluation

In this section, an example of stability analysis of a power system with a collection of connected wind turbines is evaluated using the *SSI*. The power system test case is modified from the standard three-machine, nine-bus power system from [21]. Note that the line impedances of the original system are modified such that the system becomes lossless corresponding to the formulated system equations in (10) to (17). The single-line diagram of the test system is represented in Fig. 11. The base power and voltage are at 100 MVA and 230 kV, respectively.

In this study, bus 1 is connected to an infinite bus through a tie line. Originally, the generators G2 and G3 are the synchronous generators but in this case, the generator G3 is replaced by wind power plant of 207MW, 90 of 2.3-MW DFIG wind turbines. This is the largest wind farm in Thailand [35]. The system parameters of the base case are shown in the Table 2 and the DFIG wind

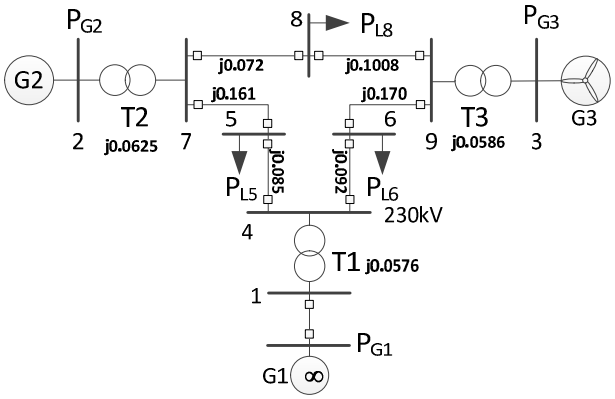

Fig. 11. Single line diagram of the modified three-machine, nine-bus power test system

Table 2. Base values of the modified 3-machine, 9-bus power test system

Bus no.	type	P (p.u.)	Q (p.u.)	V (p.u.)	Angle (radians)
Bus 1	infinite	0.716	0.27	1.04	0
Bus 2	P-V	1.63	0.067	1.025	0.162
Bus 3	P-V	0.85	-0.109	1.025	0.082
Bus 4	P-Q	0	0	1.026	-0.038
Bus 5	P-Q	1.25	0.5	0.996	-0.070
Bus 6	P-Q	0.9	0.3	1.013	-0.065
Bus 7	P-Q	0	0	1.026	0.065
Bus 8	P-Q	1	0.35	1.016	0.012
Bus 9	P-Q	0	0	1.032	0.035

Table 3. Parameters of DFIG wind turbine

	Parameters / Description	Values
M	Inertia constant (sec.)	7.0
$\bar{L}_m$	Mutual inductance (p.u.)	3.95279
$\bar{L}_r$	Rotor leakage inductance (p.u.)	0.09955
$\bar{L}_s$	Stator leakage inductance (p.u.)	0.09241
$\bar{r}_r$	Rotor resistance (p.u.)	0.00549
$\bar{r}_s$	Stator resistance (p.u.)	0.00488
k_p	Power loop constant	0.1
k_{op}	Approximated optimum power-torque constant	0.56
k_m	Approximated speed control constant	0.7
y^s_w	Speed deviation at steady state ($P_w = 1.0$)	0.2114
c_k	Frequency dependent coefficient of dynamic loads [16]	0.05

turbine parameters are shown in Table 3 [5].

5.1 System characteristics under influence of random wind power

This section represents the results of simulation and analytical analysis considering the relation between wind power, state variables, energy and LU of the power test system with the noise intensity of 0.7.

The effects of wind power (P_{G3}) variation to the exchanged power on infinite bus (P_{G1}), Energy, LU, LU_t, rotor angles on buses 2 and 3 (δ_2 , δ_3), phase angles on bus 5, 6, and 8 (θ_5, θ_6 and θ_8), and the rotor speed deviation of G3 ($\Delta\,\bar{\omega}_3$) during 100 to 720 seconds are shown in Fig. 12.

It is well-known that the state variables are related to the stability of the power system as well as the energy. From Fig. 12(a), (c), and (d), when wind power fluctuates, the angles and rotor speed deviation of G3 consequently change. However, the exchanged power on infinite bus fluctuates in the opposite direction. In Fig. 12 (b), LU highly fluctuates and changes in the reverse manner with energy while LU_t is almost steady, as a mean value of LU. In Fig. 12 (d), the rotor speed deviation (or –slip) in the range of –0.01 to 0.04 p.u. is a typical range [5].

5.2 Relation between stochastic stability index and noise intensity

This section illustrates the relation between *SSI* and noise intensity of wind power under different system

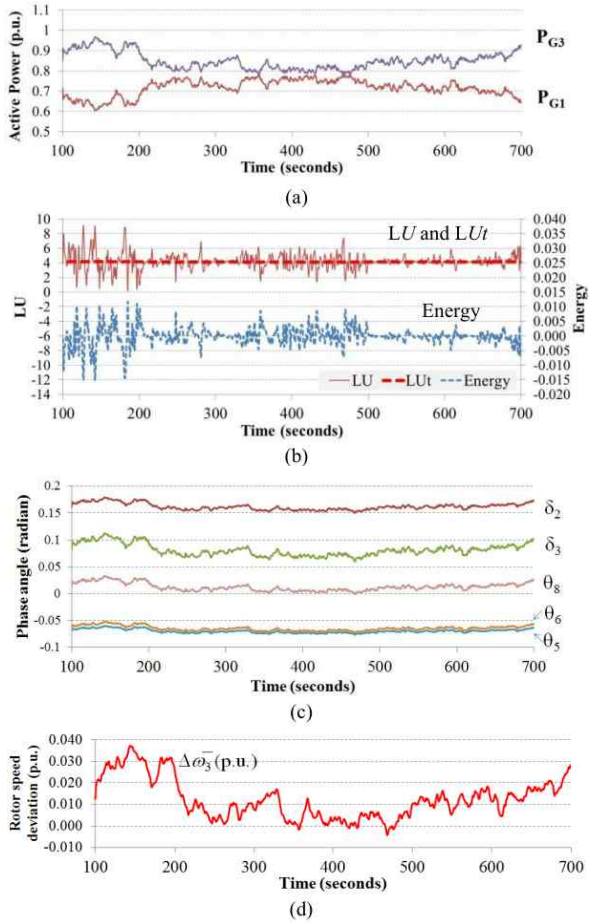

Fig. 12. (a) the active power of G1 and G3, (b) energy and its derivatives, (c) phase angles, and (d) rotor speed deviation of G3 with noise intensity of 0.7

Table 4. Test conditions with variation of P_{G2}, P_{G3}, P_{L8}, and U_c compared with the base case

Case	P_{G1} (Bus1)	P_{G2} (Bus2)	P_{G3} (Bus3)	P_{L5} (Bus5)	P_{L6} (Bus6)	P_{L8} (Bus8)	U_c
1 (base)	0.716	1.63	0.85	1.25	0.9	1	28.54
2	0.313	1.63	1.275	1.25	0.9	1	28.11
3	-0.080	1.63	1.7	1.25	0.9	1	27.39
4	-2.444	4.8	1.7	1.25	0.9	1	0.275
5	4.876	1.63	1.7	1.25	0.9	5.5	5.466

Remark: The P_{G1} is the injected power from the infinite bus.

conditions. Several events present a risk for the power system instability, for example, oversupply, overload, and high penetration of wind. Therefore, the study is evaluated under 5 test conditions focusing on the variation of wind power (P_{G3}) at different conditions of the power system including oversupply from local generator (P_{G2}), and overload from load busses (P_{L5}, P_{L6}, P_{L8}), as represented in Table 4. The effect of wind power on state variables, energy and *SSI* of the test system are analyzed.

In Table 4, Case 1 is the base case. Case 2 and Case 3 are when wind power increases to 1.275 and 1.7, respectively. For Case 4, the P_{G2} increases from 1.63 to 4.8

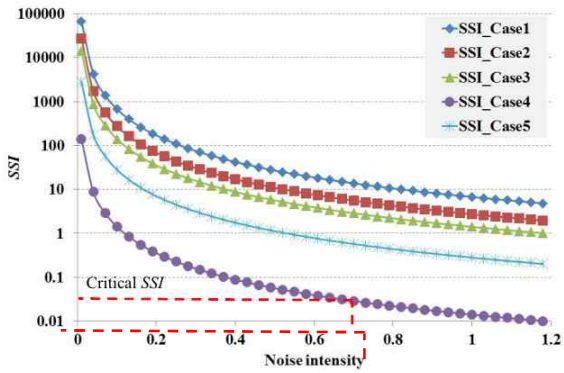

Fig. 13. The *SSI* (log scale) of the test system (Case 1 to 5) with varying noise intensities

representing an oversupply operation. For Case 5, the P_{L8} increases from 1.0 to 5.5 representing the overload operation.

The relation between *SSI* and noise intensity of wind power which varies from 0 to 1.2 is represented in Fig. 13. The steady state conditions in Table 4 are used to estimate the critical energy and LU_t which are used to calculate *SSI*.

From Fig. 13, as the noise intensity increases, the *SSI* progressively decreases. The lowest *SSI* occurs in Case 4 follows by Case 5, Case 3, Case 2, and Case 1. It implies that the power system becomes less stable when the local power system is in the oversupply mode in Case 4 and follows by the overload mode in Case 5. As the wind power increases in Cases 2 and 3, the effects on the power system stability increase reflecting through the decrease of *SSI*. In Case 4, the power system is unstable within 720 seconds as the noise intensity is more than 0.6 and at the *SSI* of about 0.04. This value can be set as the critical *SSI* for the reliability control. The *SSI* can be used as a measure of the degree of stability influenced by the random wind power. These results emphasize the advantage of the stochastic stability analysis.

5.3 Instability due to random wind power and stochastic stability index comparison

The *SSI* in the previous section is used as a measure of degree of stability of the power system under different conditions especially the oversupply mode in Case 4 causing the system to become unstable as the noise intensity is greater than 0.6. To focus on the instability case, this section presents the instability due to the random wind power. A comparison between the *SSI* and conventional stability index of Case 4 condition is given.

The simulation was done for 100 trials with 100 series of random values of wind power at a specified noise intensity and mean wind power. For illustration purpose, the samples of operation in Case 4 with the noise intensity of 0.7 are shown in Fig. 14. The system energy, the phase angle on bus 2, and the frequency deviation on bus 3 are displayed in Fig. 14 (a), (b), and (c), respectively.

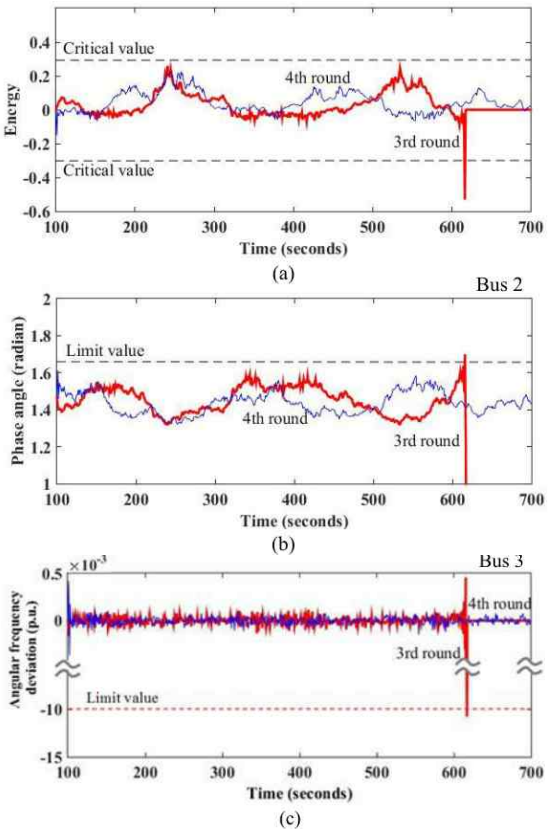

Fig. 14. (a) energy, (b) bus 2 phase angles, and (c) bus 3 angular frequency deviation of Case 4 with noise intensity of 0.7 of 3rd round and 4th round

From Fig. 14, the 3rd and 4th rounds of simulation with different trajectories of state variables provide different results of power system stability due to the stochastic behavior. For example, the 3rd round simulation results show that, at 617 seconds, the bus 2 phase angle and bus 3 angular frequency reach their limits at 1.6 radian and 1%, respectively. It is implied that when the wind power changes, the state variables vary over their limit values causing the energy to deviate beyond the critical value. However, the instability is not observed in the results of 4th round simulation. This indicates a possibility that the system exhibits instability behavior due to the random effect of the wind power even though the operating condition remains the same.

For each noise intensity in a particular initial condition the wind power is generated randomly and the simulation is carried out until the state variables of interest (speed and angle) are out of the limit or exit the predefined boundary. The first exit times are determined for 100 trials of simulation and the mean value is of the first exit times is obtained.

When the noise intensity increases in Case 4, the mean first exit time decreses with the reduction of *SSI*, as shown in Table 5.

From the results in Table 5, it implies that the power system has higher possibility of becoming unstable with

Table 5. Mean first exit time, *SSI*, and computational time in Case 4

Noise intensity	Security Index		Computational time (sec.)	
	MFET	*SSI*	MFET	*SSI*
0.7	310.3	0.0289	956.9	0.109
0.8	279.2	0.0222	927.3	0.062
0.9	243.5	0.0175	873.0	0.078
1.0	227.7	0.0142	647.7	0.094
1.1	221.8	0.0117	1216.3	0.140
1.2	205.2	0.0098	954.7	0.125

*Remark: MFET is the mean first exit time from 100 trials.

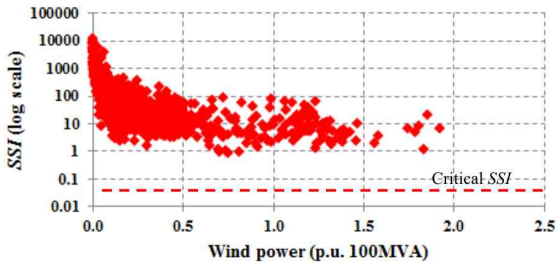

Fig. 15. The *SSI* of the test system of Case 4 with varied wind power of geographically distributed wind turbines

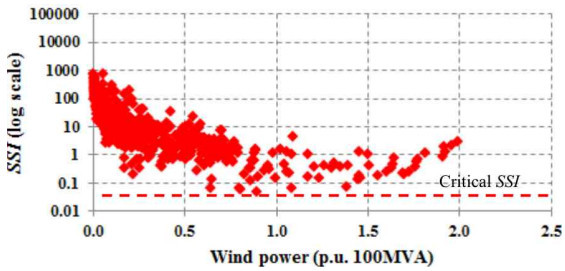

Fig. 16. The *SSI* of the test system of Case 4 with varied wind power using aggregated model of wind turbines

shorter time span when the noise intensity is increased. Evidently, the *SSI* can reresent an influence of noise intensity of wind power to the power system stability similar to the mean first exit time with less computational effort. Excluding the process of obtaining the system initial conditions in power flow analysis, the computation of mean first exit time of 100 trials require 647.7 to 1,216.3 seconds while the *SSI* computation requires less than 0.2 seconds on an IntelR CoreTM i7 4510U CPU at 2.0 GHz with 4.0GB of RAM.

5.4 *SSI* Implementation and analysis

From Figs. 6 and 7, the *SSI* of the test system under an oversupply condition (Case 4 with varied wind power) can be determined using measured wind data as represented in Figs. 15 and 16, respectively.

In Fig. 15, the lowest *SSI* of 0.87 occurs at 0.75 p.u. of wind power. The value of *SSI* is much larger than the

critical *SSI* of 0.04. This means that the power system is rather robust under the specified condition. However in Fig. 16, the lowest *SSI* of 0.05 at wind power of 0.90 p.u. is much close to the critical *SSI* which implies that the power system is less robust for wind power plant with aggregated model. As mentioned earlier, an increase of wind power and its noise intensity has more influence on *SSI*. From measured wind data, the noise intensity decreases with an increase of wind power. From these results, the degree of influence of wind power affecting the power system stability depends on the characteristics of wind power deviation and the condition of the power system. The *SSI* provides insight in quantifiable effects of random wind power.The *SSI* can be used to evalutate or even forecast the stability of the power system using statistical wind data.

6. Conclusions

This paper proposes the Stochastic Stability Index (*SSI*) which is implemented on the modified three-machine, nine-bus power test system incorporating wind power from DFIG wind turbines. The random effects of wind power have been characterized where a hypothesis test has confirmed that the wind power of geographically distributed wind turbines is normally distributed. The *SSI* is computed from the critical energy and the derivative of the relative well-defined energy. The results of analysis reveal that the *SSI* is obviously corresponding to the mean exit time. The *SSI* decrease with increasing of wind power and its noise intensity and with the over and under supply conditions of the power system. This situation occurs with the same direction as the mean exit time when the state variables out of the limit values. However, the solution of mean exit time is computationally expensive. For the power test system proposed in this study, it spends less than 0.2 second to compute the SSI for each test condition while the computation of mean exit time from 100 trials spend 647.7 to 1,216.3 seconds. Therefore, *SSI* can be used to evaluate the stability of the power system comparatively with much less computational effort. The period of short term wind power forecast typically spans from few minutes to several hours ahead. Therefore, the *SSI* computation process can be implemented rapidly following the forecasting processes with less effect to the overall time frame of correct variation of regulating reserve.

Acknowledgements

This work was supported by the Joint Graduate School of Energy and Environment (JGSEE), CES Solar Cells Testing Center (CSSC), Department of Electrical Engineering, Faculty of Engineering, King Mongkut's University of Technology Thonburi (KMUTT).

Nomenclature

$\bar{P}_m$	mechanical power (p.u.)
$\bar{P}_e$	electromagnetic power (p.u.)
$\bar{P}_l$	load power (p.u.)
M, D	Inertia and damping constants of generator (sec.)
α_w	noise intensity of the wind power
$\dot{W}$	zero-mean Gaussian distributed white noise
ω_0	fundamental angular frequency (p.u.)
ω_r	angular speed of rotor (electrical radians per second)
ω_s	angular speed of electrical field at stator (electrical radians per second)
$\Delta\bar{\omega}_w$	rotor speed deviation (p.u.)
$\Delta\bar{\omega}_i$	speed deviation of synchronous generator (p.u.)
s_w	slip of the induction generator
$\bar{\mathbf{V}}_s$	stator voltage in x-y axis (p.u.)
$\bar{\mathbf{V}}_r$	rotor voltage in x-y axis (p.u.)
$\bar{V}_{rd}$, $\bar{V}_{rq}$	direct-quadrature (d-q) components of $\bar{\mathbf{V}}_r$ (p.u.)
$\bar{V}$	voltage bus (p.u.)
$\bar{\mathbf{E}}$'	voltage behind transient reactance in x-y axis (p.u.)
$\lvert\bar{E}'\rvert$	magnitude of $\bar{\mathbf{E}}$' (p.u.)
δ_w	angle of $\bar{\mathbf{E}}$' (radians)
δ'_w	angle between $\bar{\mathbf{E}}'_w$ and $\bar{\mathbf{V}}_{sw}$ (radian)
δ_i	rotor angle of synchronous generator (radian)
θ_k	phase angle of the load bus voltages (radian)
θ_j	angle of bus voltage j (radian)
$\bar{\mathbf{I}}_s$	stator current in x-y axis (p.u.)
$\bar{I}_{sd}$, $\bar{I}_{sq}$	direct-quadrature (d-q) components of $\bar{\mathbf{I}}_s$ (p.u.)
c_k	frequency dependent coefficient of dynamic loads
$\bar{X}'$	transient reactance (p.u.)
$\bar{X}$	open-circuit reactance on stator (p.u.)
$\bar{T}_0$	the transient open-circuit time constant (seconds)
$\bar{r}_r$	rotor resistance (p.u.)
$\bar{L}_m$	mutual inductance (p.u.)
$\bar{L}_{rr}$	sum of mutual and rotor leakage inductances (p.u.)
$\bar{L}_{ss}$	sum of mutual and stator leakage inductances (p.u.)
k_a , c_a	slope and offset of the linear relationship between δ_w and δ'_w
$\bar{T}_{sp}$	set-point torque at any generator speed (p.u.)
k_{op}	aerodynamic performance constant from manufacturer
k_{c1} , k_{c2}	turbine generator constants
k_m	approximated speed control constant
k_p , k_w	speed-torque control parameters (PI-controller) of the turbine generator
$\bar{B}_{wj}$, $\bar{B}_{ij}$, $\bar{B}_{kj}$	susceptances between bus w , i, and k, and bus j (p.u.)
x_w $(=\delta_w)$	angle of voltage behind transient reactance (radian)
y_w $(=\Delta\bar{\omega}_w)$	speed deviation of DFIG (p.u.)
x_i $(=\delta_i)$	rotor angle of the synchronous generator (radian)
y_i $(=\Delta\bar{\omega}_i)$	speed deviation the synchronous generator (p.u.)

x_k ($=\theta_k$) phase angle of the voltages at load buses k (radian)
y_0 speed deviation at the infinite bus (p.u.)
U relative well-defined energy function
$u(\mathbf{X},t)$ stochastic well-defined energy function
LU stochastic differential function of U
LU_t trace function of U
U_c critical energy
$G(x,t)$ diffusion function
$f(x,t)$ nonlinear drift function

References

[1] U.S. Department of Energy (DOE), *2016 Wind Technologies Market Report*, August 2017.

[2] Global Wind Energy Council (GWEC), *Global Wind Report: Annual Market Update 2016*.

[3] Joint Research Centre(JRC), *JRC Wind Energy Status Report 2016 Edition*, 2017.

[4] J.L. Rueda and F. Shewarega, "Small Signal Stability of Power Systems with Large Scale Wind Power Integration," *in Proceedings of XIII Eriac Decimo Tercer Encuentro Regional Iberoamericano De CIGRÉ*, Puerto Iguazu, Argentina, May 2009.

[5] Olimpo Anaya-Lara, Nick Jensens, Janaka Ekanayake, Phill Cartwright, Mike Hughes, *Wind Energy Generation Modeling and Control*, John Wiley & Sons Ltd., UK, 2009.

[6] T.R. Ayodele , A.A. Jimoh , J.L Munda, J.T Agee, "The Influence of Wind Power on the Small Signal Stability of a Power System," *in Proceedings of International Conference on Renewable Energies and Power Quality (ICREPQ'11)*, Las Palmas, Spain, April 2011.

[7] S.Q. Bu, W. Du, H. F. Wang, Z. Chen, L. Y. Xiao and H. F. Li, "Probabilistic Analysis of Small-signal Stability of Large-scale Power Systems as Affected by Penetration of Wind Generation," *IEEE Transactions on Power Systems*, Vol. 27, No. 2, May 2012.

[8] R.C. Burchett and G. T. Heydt, "Probabilistic Methods for Power System Dynamic Stability Studies," *IEEE Transactions on Power Apparatus and Systems*, Vol. PAS-97, no. 3, May/June 1978.

[9] Bo Yuan, Ming Zhou, Gengyin Li, and Xiao-Ping Zhang, "Stochastic Small-Signal Stability of Power Systems With Wind Power Generation," *IEEE Transactions on Power Systems*, Vol. 30, July 2015.

[10] R. Billinton and W. Li, *Reliability assessment of electric power systems using Monte Carlo methods*, New York: Plenum Press, 1994.

[11] Z. Xu, Z. Y. Dong, and P. Zhang, "Probabilistic Small Signal Analysis using Monte Carlo Simulation," *in Proceedings of Power Engineering Society General Meeting*, IEEE, vol. 2, pp. 1658-1664, June 2005.

[12] Theresa Odun-Ayo, and Mariesa L. Crow, "Structure-Preserved Power System Transient Stability Using Stochastic Energy Functions," *IEEE Transactions on Power Systems*, vol. 27, no. 3, August 2012.

[13] J.M. Morales, L. Baringo, A.J. Conejo, and R. Minguez, "Probabilistic power flow with correlated wind sources," *IET Gener. Transm. Distrib.*, vol. 4, Iss. 5, pp. 641-651, 2010.

[14] Changjiang Jiang, Wei Zhao, Junyong Liu, Wuxing Liang, Bazargan Masoud, Xiaohui Lu, Tao Luo, Tao Meng, "A New Numerical Simulation for Stochastic Transient Stability Analysis of Power Systems Integrated Wind Power," *in Proceedings of International Conference on Power System Technology (POWERCON 2014)*, Chengdu, China, Oct. 2014.

[15] Wei Wu, , Keyou Wang, Guojie Li, and Yue Hu, "A Stochastic Model for Power System Transient Stability with Wind Power," *in Proceedings of PES General Meeting | Conference & Exposition 2014*, IEEE, 27-31 July 2014.

[16] C.O. Nwankpa, S.M. Shahidehpour , "A stochastic model for small disturbance stability analysis of electric power systems, *Electrical Power & Energy Systems*, vol. 13, no. 3., 1991.

[17] Hadiza Mohammed, Chika O. Nwankpa, "Stochastic Analysis and Simulation of Grid-Connected Wind Energy Conversion System," *IEEE Transactions on Energy Conversion*, vol. 15, no. 1, Mar 2000.

[18] Anawach Sangswang and Chika O. Nwankpa, Member IEEE, "Effects of Switching-Time Uncertainties on Pulsewidth-Modulated Power Converters: Modeling and Analysis," *IEEE Transactions on Circuits and Systems-I: Fundamental Theory and Applications*, vol. 50, no. 8, August 2003.

[19] Zeev Schuss, *Theory and Applications of Stochastic Processes: An Analytical Approach*, New York : Springer, 2010.

[20] P. Parinya, A. Sangswang, K. Kirtikara, D. Chenvidhya, S. Naetiladdanon, C. Limsakul, "A Study of Impact of Wind Power to Power System Stability using Stochastic Stability Index," *in Proceedings of 2014 IEEE International Symposium on Circuits and Systems (ISCAS 2014)*, Melbourne, Australia, June 2014.

[21] P. W. Sauer and M. A. Pai, *Power System Dynamic and Stability*. New Jersey: Prentice Hall, 1998.

[22] Tony Burton, David Sharpe, Nick Jenkins, Ervin Bossanyi , *Wind Energy Handbook*, John Wiley & Sons, 2001.

[23] Isac Van der Hoven, "Power spectrum of horizontal wind speed in the frequency range from 0.0007 to 900 cycles per hour," *Journal of Meteorology*, vol. 14, pp. 160-4, 1956.

[24] Pedro Rosas, *Dynamic Influences of Wind Power on The Power System*, a Thesis document, Technical University of Denmark, 2003.

[25] Lulian Munteanu, Antoneta Luliana Bratcu, Nicoloas-Antonio Cutululis, Emil Ceanga, *Optimal Control of Wind Energy Systems, Advances in Industrial Control*, Springer-Verlag London Limited, UK, 2008.
[26] Louie Henry, "Characterizing and modeling aggregate wind plant power output in large systems," *in Proceedings of IEEE Power and Energy Society General Meeting*, Minesota, USA, July 2010.
[27] George J. Anders, *Probability Concepts in Electric Power Systems*, John Wiley & Sons, 1990.
[28] National Renewable Energy Laboratory (NREL), *Long-Term Wind Power Variability*, Technical Report No. NREL/TP-5500-53637, January 2012.
[29] Atsushi Ishigame and Tsuneo Taniguchi, "Transient Stability Analysis for Power System Using Lyapunov Function with Load Characteristics," *in Proceeding of Power Engineering Society General Meeting, IEEE,* July 13-17, 2003.
[30] Glenn W. Stagg and Ahmed H. El-Abiad, *Computer methods in power system analysis*, McGraw-Hill, 1968.
[31] Hsiao-Dong Chiang, *Direct Methods for Stability Analysis of Electric Power Systems : Theoretical Foundation, BCU Methodologies, and Applications*, John Wiley & Sons Ltd., UK., 2011.
[32] M. A. Pai, *Power System Stability Analysis by the Direct Method of Lyapunov*, North-Holland Publishing Company, Amsterdam, 1981.
[33] M. Ribbens-Pavella, B. Lemal, "Fast determination of stability regions for online transient power-system studies," *PROC. IEE*, Vol.123, No.7, 1976.
[34] Measurement and Control Laboratory, *Stochastic Systems*, Swiss Federal Institue of Technology Zurich, April 14, 2011.
[35] Phil Napier-Moore, "Producing wind power in Thailand: Industry status and challenges," *in Proceeding of Renewable Energy Asia 2014*, June 4, 2014.

Panom Parinya He was born in Phayao, Thailand. He received the B.Eng. degree from the Kasetsart University (KU), Bangkok, Thailand in 2003 and the M.S. degree from the Joint Graduate School of Energy and Environment (JGSEE), King Mongkut's University of Technology Thonburi (KMUTT), Thailand, in 2007. Since 2008, he was a Researcher with the CES Solar Cells Testing Center (CSSC), KMUTT. His research interests are wind and solar energy assessment, impacts of wind and solar energy on the power system, probabilistic methods for power system stability evaluation, PV system testing and analysis.

Krissanapong Kirtikara He was born in Bangkok, Thailand. He received the B.Eng. first-class honours degree and Ph.D. degree from the University of Glasgow, UK in 1969 and 1973, respectively. After that, he started his work as lecturer and researcher with KMUTT. He is currently a researcher, lecturer, and advisor to the university. His research interests include solar radiation assessment and modeling, solar cells and systems characterization, standalone systems, grid-connected PV systems, RE policy and management.

Anawach Sangswang He was born in Bangkok, Thailand. He received the B.Eng. degree from the King Mongkut's University of Technology Thonburi (KMUTT), Bangkok, Thailand in 1995 and the M.S. and Ph.D. degrees from Drexel University, Philadelphia, PA, in 1999 and 2003, respectively. From 1999 to 2003, he was a Research Assistant with the Center for Electric Power Engineering, Drexel University. He is currently an Assistant Professor with the Department of Electrical Engineering, KMUTT. His research interests include stochastic modeling, digital control of power electronic converters, and power system stability.

Dhirayut Chenvidhya He was born in Bangkok, Thailand. He received the B.Eng., M.Eng. in Electrical Engineering, and the Doctor of Engineering in Energy Technology from the King Mongkut's University of Technology Thonburi (KMUTT), Bangkok, Thailand, in 1991, 1993 and 2003, respectively. He is now the Director of the CES Solar Cells Testing Center (CSSC) of the KMUTT. His main research areas include solar cells characterization, standard testing and PV systems analysis. His publications were published as chapter in textbooks, international journals and international conferences more than 50 articles.